Power Converter-based Three-phase Induction Motor Load Emulator

Jing Wang, Yiwei Ma, Liu Yang, Leon M. Tolbert, Fred Wang

Center for Ultra-Wide-Area Resilient Electric Energy Transmission Networks (CURENT)
The University of Tennessee
Knoxville, TN USA 37996-2250

***Abstract* — A three-phase induction motor emulator using power electronic converters is introduced in this paper. The emulator is intended to be used in an ultra-wide-area grid transmission network emulator represented by regenerative converters structure. The load emulator converter is controlled in rectifier mode to behave like the real induction motor load, whose model is described and programmed in the digital controller. This paper discusses specifically about the induction motor dynamic modeling, numerical method used in the controller, and finally experimental result verification of starting up transient.**

***Index Terms* — Hardware testbed, regenerative converter, ultra-wide-area transmission network emulator, power electronic load, control algorithms, Runge-Kutta method, starting up transient, dynamic performance**

I. INTRODUCTION

Power electronic converter could be controlled to emulate various kinds of dynamics in flexible ways [3-5, 7]. It could behave almost exactly like the model described in its controller whose time scale is much longer than the controller reacting time.

The induction motor, for example, has the typical dynamics time scale of around several seconds or hundreds of milliseconds. The power converter could react quickly to the reference changes, usually within tens of milliseconds or even several milliseconds. So the power converter is fast enough in voltage-current relations compared with that of a three-phase induction motor to represent its behavior. This comparison could be applied to most of the power system components, which means that the generators, induction motors, renewables, most kinds of loads, etc. can be represented by power electronic converters. The structure of power converter emulator is presented in Fig. 1. By flexibly programming power system component electrical relations inside a controller, current/voltage command representing dynamics of a component model inside could be calculated to work as references for the converter to track. Then, the power converter could behave exactly as designed, and by combining different kinds of emulators together, various scenarios of simulations could be initiated and studied [2].

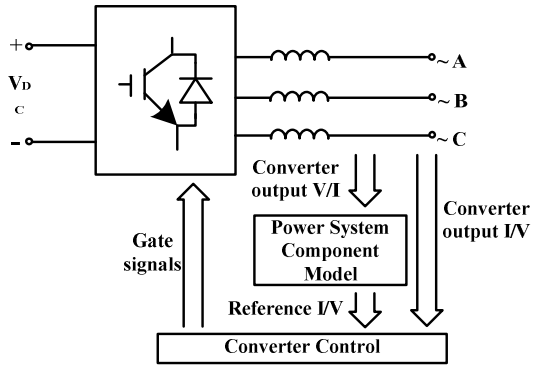

Figure 1. Power converter emulator structure.

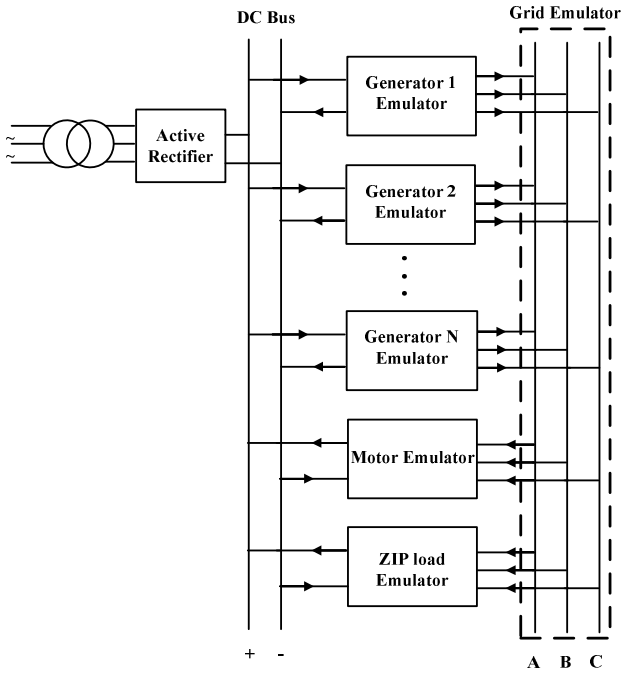

Figure 2. Proposed grid emulation system structure.

Fig. 2 shows the architecture of the power electronic converter based scaled hardware test-bed (HTB), which emulates the power system performances with inter-connected emulators [2]. This universal hardware testbed will be established to match the real power system components. With it, various kinds of advanced and state-of-art technology could be tested and verified by changing the configuration or controller models. Meanwhile, different network and scenarios of power system dynamics could be analyzed and emulated through the test-bed.

In order to perform like actual power system components, a robust control scheme should be built in the emulator controller in order to imitate the actual dynamics [4, 6]. Different from conventional loads, power electronic loads in HTB offer the option of demand and supply power on the grid emulator side while circulating it on the DC side, which is especially beneficial when working under high power condition.

In this paper, the motor load emulator design procedure is discussed in detail.

II. Emulator Structure

Three-phase induction motor is a very common large power system load. Its dynamic transient performance could induce power system voltage and frequency fluctuations. So an accurate emulator representing its dynamic behavior is crucial to the system's overall simulation.

The electrical inputs to a three phase induction motor are three-phase AC stator voltage V_{abc} and electrical frequency ω, and electrical outputs are three-phase currents I_{abc}. The electrical characteristics are also determined by the mechanical relations between torque T and rotating speed ω_r.

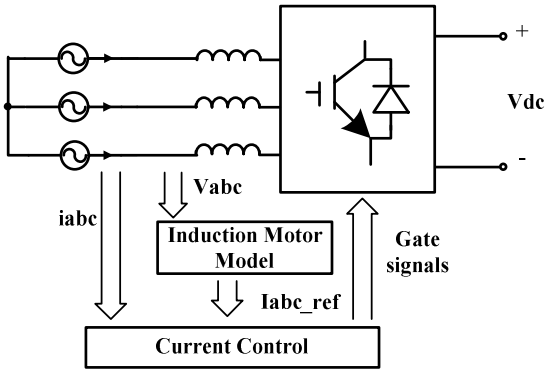

Figure 3. Induction motor load emulator structure.

As illustrated in Fig. 4, the calculation begins from sampling of three phase voltage V_{abc}. After PLL operation, frequency and angle are obtained and used as dq transformation angle reference.

The induction motor model is described in dq domain with relations among voltage, current, flux, torque, inertia and rotating speed. After each iteration cycle, i.e. each PWM calculation period in the DSP, references of three phase currents would be deduced and used as commands for the current controller to track. Finally gate signals are generated accordingly and fed to the converter.

III. Three Phase Induction Motor Model

The motor model equations are using the reference frame of synchronous rotating speed so that input voltages are all constants in the dq domain.

Equations (1) - (3) are the model equations describing electromagnetic and electromechanical relations between flux, current, voltage and rotation speed (all in per unit

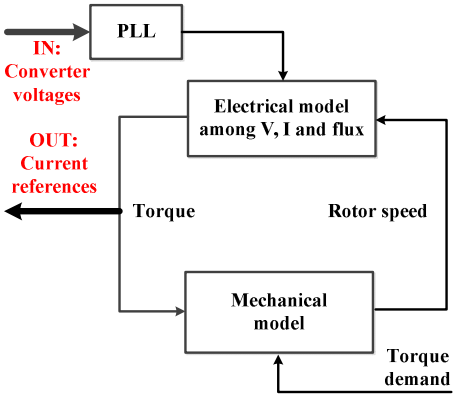

Figure 4. Induction motor load model structure.

value) [1, 8, 9]. The variables are defined as: v_{qs}, v_{ds} and v_{0s} are stator voltage transformed in dq0 domain, v_{qr}, v_{dr} and v_{0r} are rotor voltage transformed in dq0 domain, ω is angular speed of reference frame, ω_r is rotating angular speed of the motor, r_s and r_r are stator and rotor resistances, X_{ls} and X_{lr} are stator and rotor leakage reactance, X_{ss} and X_{rr} are stator and rotor reactance, X_M is magnetizing reactance, p is pole pair number, λ_{qs} and λ_{ds} are q and d axis flux for stator, i_{qs} and i_{ds} are currents on q and d axis for the stator, H is inertia constant of motor.

The parameters used in this model are corresponding to a very large squirrel cage induction motor (per unit values): r_s = 0.0197, r_r = 0.0184, X_{lr} = 0.2848, X_{ls} = 0.3267, X_m = 10.3153, p = 3, H = 0.1316.

Equation (1) contains derivative variables and thus requires using a numerical method during each iteration cycle for system stability and accuracy. Thus equation (1) could be concluded in the form of numerical iteration form shown below in (4)

$$\frac{d}{dt}\vec{y} = A \cdot \vec{y} + b \tag{4}$$

with vector y to be solved: $\vec{y} = [i_{qs} \quad i_{ds} \quad i_{0s} \quad i_{qr} \quad i_{dr} \quad i_{0r}]^T$.

Matrices ***A*** and ***b*** could be deduced from (1), and not repeated here. The numerical method applied is explicit Runge-Kutta 4th order:

$$\frac{d}{dt}\vec{y} = f(t, \vec{y}), \qquad \vec{y}(t_0) = 0 \tag{5}$$

$$\vec{y}_{n+1} = \vec{y}_n + \frac{1}{6}(k_1 + 2k_2 + 2k_3 + k_4) \tag{6}$$

where

$$k_1 = \Delta t \cdot f(t_n, \vec{y}_n)$$

$$k_2 = \Delta t \cdot f(t_n + \frac{1}{2}\Delta t, \vec{y}_n + \frac{1}{2}k_1)$$

$$k_3 = \Delta t \cdot f(t_n + \frac{1}{2}\Delta t, \vec{y}_n + \frac{1}{2}k_2)$$

$$k_4 = \Delta t \cdot f(t_n + \Delta t, \vec{y}_n + k_3)$$

$$\begin{bmatrix} v_{qs}^{pu} \\ v_{ds}^{pu} \\ v_{0s}^{pu} \\ v_{qr}^{pu} \\ v_{dr}^{pu} \\ v_{0r}^{pu} \end{bmatrix} = \begin{bmatrix} r_s^{pu} & \omega^{pu}\cdot X_{ss}^{pu} & 0 & 0 & -\omega^{pu}\cdot X_M^{pu} & 0 \\ -\omega^{pu}\cdot X_{ss}^{pu} & r_s^{pu} & 0 & -\omega^{pu}\cdot X_M^{pu} & 0 & 0 \\ 0 & 0 & r_s^{pu} & 0 & 0 & 0 \\ 0 & (\omega^{pu}-\omega_r^{pu})\cdot X_M^{pu} & 0 & r_r^{pu} & (\omega^{pu}-\omega_r^{pu})\cdot X_{rr}^{pu} & 0 \\ -(\omega^{pu}-\omega_r^{pu})\cdot X_M^{pu} & 0 & 0 & -(\omega-\omega_r)\cdot X_{rr} & r_r^{pu} & 0 \\ 0 & 0 & 0 & 0 & 0 & r_r^{pu} \end{bmatrix} \cdot \begin{bmatrix} i_{qs}^{pu} \\ i_{ds}^{pu} \\ i_{0s}^{pu} \\ i_{qr}^{pu} \\ i_{dr}^{pu} \\ i_{0r}^{pu} \end{bmatrix}$$

$$+ \begin{bmatrix} X_{ss}^{pu} & 0 & 0 & X_M^{pu} & 0 & 0 \\ 0 & X_{ss}^{pu} & 0 & 0 & X_M^{pu} & 0 \\ 0 & 0 & X_{ls}^{pu} & 0 & 0 & 0 \\ X_M^{pu} & 0 & 0 & X_{rr}^{pu} & 0 & 0 \\ 0 & X_M^{pu} & 0 & 0 & X_{rr}^{pu} & 0 \\ 0 & 0 & 0 & 0 & 0 & X_{lr}^{pu} \end{bmatrix} \cdot \frac{1}{\omega_b} \cdot \frac{d}{dt} \begin{bmatrix} i_{qs}^{pu} \\ i_{ds}^{pu} \\ i_{0s}^{pu} \\ i_{qr}^{pu} \\ i_{dr}^{pu} \\ i_{0r}^{pu} \end{bmatrix} \quad (1)$$

$$T_e = \left(\frac{3}{2}\right)\left(\frac{P}{2}\right)(\lambda_{ds} i_{qs} - \lambda_{qs} i_{ds}) \quad (2)$$

$$\omega_r = \int_0^t \frac{T - T_L - T_{fri}}{2H} d\tau \quad (3)$$

Every iteration is accomplished within a switching cycle using TI DSP TMS320F28335, with calculation procedure shown as (5) – (6).

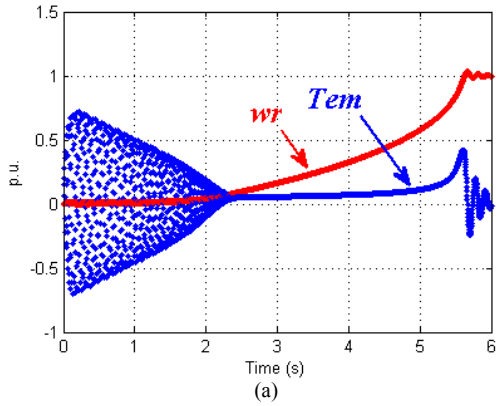

(a)

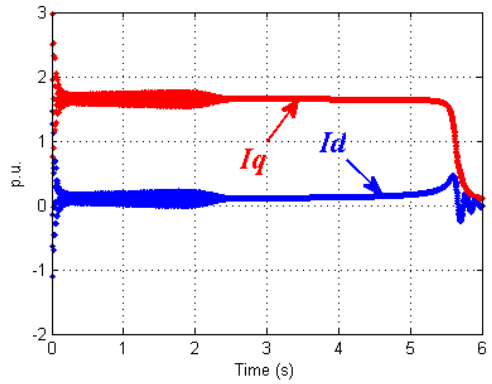

(b)

Figure 5. Motor model outputs with ideal voltage and frequency inputs
(a) electromechanical torque,
(b) start-up currents in dq domain.

By calculating the motor model with stable voltage inputs and frequency, the waveforms of three phase currents output and mechanical torque and speed outputs with free start-up acceleration could be shown in Fig. 5.

With ideal voltage and frequency inputs, the induction motor model starts up with smooth fluctuation transients. The starting up current for an induction motor in dq domain could be as high as 2-3 times that of normal rated current. The starting up time takes around 5.5 s under this case.

IV. Experimental Results

The experiment was implemented using the converter configuration shown in Fig. 6. The test setup is using two paralleled converters: the above one is controlled as an inverter to regulate the three phase voltage V_{abc} [10]. Voltage

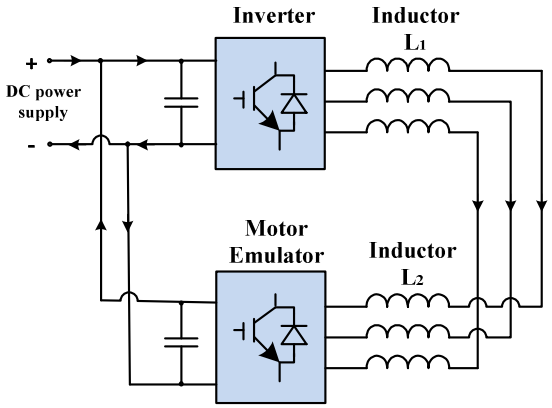

Figure 6. Converter parallel testing configuration.

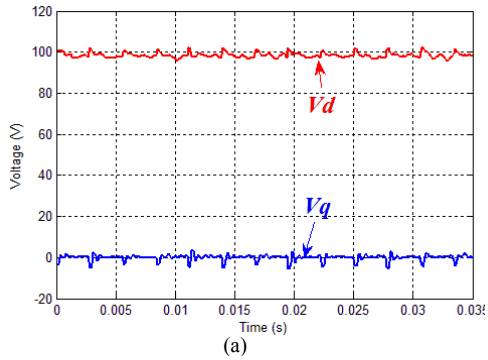

(a)

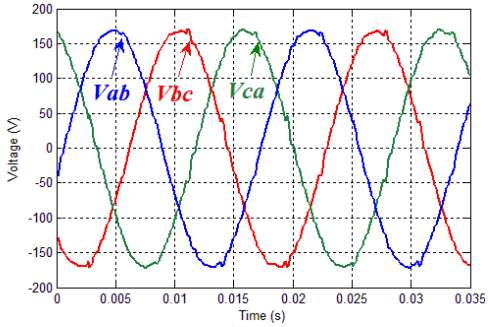

(b)

Figure 7. Inverter output three phase voltage
(a) in dq domain (in Park's transformation);
(b) in abc domain.

references are: V_d 100 V and V_q 0 V. Output inductor filter L_1 is 0.5 mH. The bottom converter input three phase currents I_{abc} are controlled to track the references from motor model implanted in the controller, current base references (before starting of motor model) are: I_d 10 A and I_q 5 A. The output inductor filter L_2 is 1 mH.

The experiment starting up procedure is: (1) starting up both converters running in parallel; (2) giving motor emulator constant current reference bases first to enable the configuration running; (3) then after giving a trigger signal, the induction motor begins free acceleration starting up process; in the meantime, the converter is controlled by a classical PI controller programmed inside the DSP to track the current references calculated.

The circulating current within a switching cycle between paralleled converters was suppressed by synchronization of the carrier waveforms using CAN bus communication in the DSP.

The three-phase voltage outputs regulated by the inverter are shown in Fig. 7. In the experiment, V_{dc} increases to 250 V and V_d is regulated to 100 V while V_q is 0 V (using Park's dq0 transformation). Three phase voltage inputs to motor emulator is shown in Fig. 7(b). The detailed control and implementation for the voltage control design could be found in [10].

After pushing the trigger button to enable induction motor starting up, the motor model is then calculated during each PWM period inside the DSP. The torque and rotating speed performances of the motor model are shown in Fig.

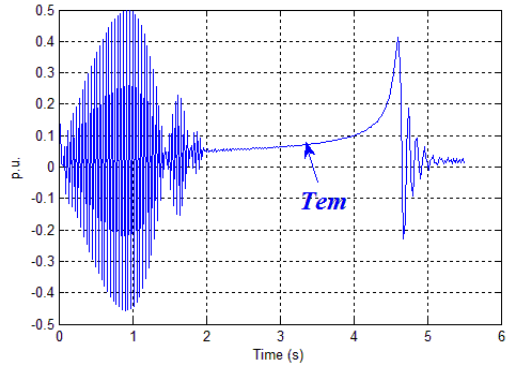

(a)

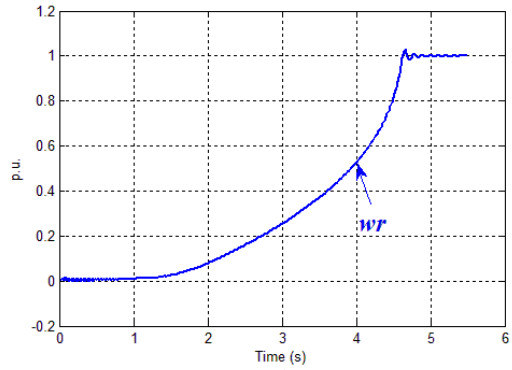

(b)

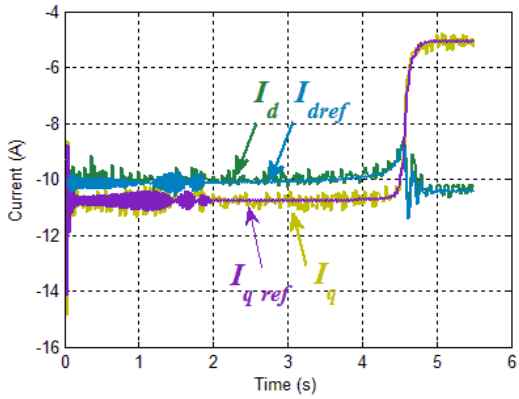

(c)

Figure 8. Induction motor model starting up transient results record in DSP:
(a) mechanical torque; (b) mechanical rotating speed;
(c) starting up current in dq domain comparison between references and real outputs (in converter dq0 transformation).

8(a) and (b) indicating the process of rotor model rotating from zero speed to full speed. Current outputs from the emulator and references in dq domain are also compared in Fig. 8(c). The current references are obtained by adding base current values with the starting up currents of the induction motor model. One of the three phase current I_a overall shape is illustrated in Fig. 9 revealing the starting up current inrush transient of induction motor.

As compared with motor model starting up with ideal voltage and frequency inputs shown in Fig. 5, it is observed that the transient is a little different in the time duration and

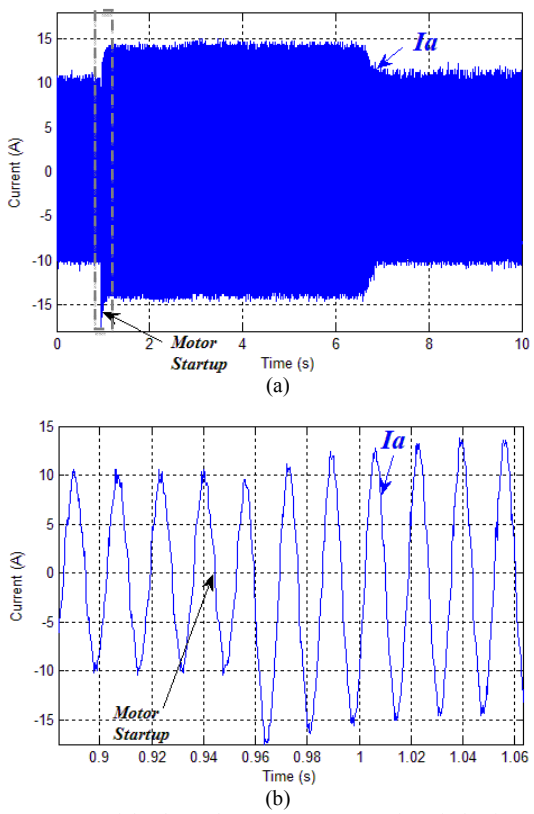

Figure 9. One of the three phase current outputs from induction motor emulator converter in abc domain:
(a) overall motor starting up current for one phase;
(b) close-up for partial waveform at starting transient.

partial shape. This is because the voltage in the experiment is controlled in the real-time situation, and there are voltage and frequency fluctuations and minor variations causing the transient to not be that 'smooth' as in the ideal case.

V. Conclusion

Power converter based induction motor emulator is designed and verified in this paper. The dynamic three-phase induction machine model was programmed using Runge-Kutta numerical method in the DSP28335. The experiments successfully demonstrated that the power converter emulator could track and represent the induction motor with appropriate design of control parameters.

This induction motor emulator can be used in the whole hardware testbed system for various purposes of power system scenario emulation.

Acknowledgement

This work was supported primarily by the Engineering Research Center Program of the National Science Foundation and the Department of Energy under NSF Award Number EEC-1041877 and the CURENT Industry Partnership Program.

References

[1] Paul C. Krause, Oleg Wasynczuk and Scott D. Sudhoff, *Analysis of Electric Machinery and Drive Systems*, Second Edition, Purdue University, 2002.

[2] J. Wang, L. Yang, Y. Ma, X. Shi, et al, "Regenerative Power Converters Representation of Grid Control and Actuation Emulator." *IEEE Energy Conversion Congress and Exposition*, Sep. 15-20, 2012, pp. 2460-2465.

[3] H. Slater, D. Atkinson, and A. Jack, "Real-time emulation for power equipment development. Part II: The virtual machine," *Proc. Inst. Elect. Eng.*, vol. 145, no. 3, pp. 153–158, May 1998.

[4] M. Armstrong, D. J. Atkinson, A. G. Jack, and S. Turner, "Power system emulation using a real time, 145 kW, virtual power system," in *Proc. Eur. Conf. Power Electron. Appl.*, 2005, 10 pp. - P.10.

[5] A. Emadi and M. Ehsani, "Multi-converter power electronic systems: definition and applications," in *Proc. IEEE 32nd Power Electron. Spec. Conf.*, Vancouver, BC, Canada, Jun. 2001, pp. 1230–1236.

[6] A. Emadi, "Modeling of power electronic loads in AC distribution systems using the generalized state space averaging method," *IEEE Trans. Ind. Electron.*, vol. 51, no. 5, pp. 992–1000, Oct. 2004.

[7] Y. Srinivasa Rao and Mukul Chandorkar, "Electrical load emulation using power electronic converters," *Proceedings of the IEEE International Conference on Industrial Technology*, Gippsland, Australia, 19-21 November 2008, pp. 1-6.

[8] K. L. Shi, T. F. Chan, Y. K. Wong, and S. L. Ho, "Modeling and simulation of an induction motor," *Int. J. Elect. Eng. Educ.*, vol. 36, no. 2, pp. 163–172, 1999.

[9] P. Kundur, *Power System Stability and Control*. New York: McGrawHill, 1994.

[10] L. Yang, X. Zhang, Y. Ma, et al, "Hardware Implementation and Control Design of Generator Emulator in Multi-Converter System. " *The Applied Power Electronics Conference and Exposition,* Mar 17-21, 2013.